Vascular Tissue-Specific Expression of *Bnac4.BOR1;1c*, an Efflux Boron Transporter Gene, is Regulated in Response to Boron Availability for Efficient Boron Acquisition in *Brassica Napus*

Sheliang Wang
Huazhong Agricultural University
Ling Liu
Huazhong Agricultural University
Dan Zou
Huazhong Agricultural University
Yupu Huang
Huazhong Agricultural University
Zhe Zhao
Huazhong Agricultural University
Guangda Ding
Huazhong Agricultural University
Hongmei Cai
Huazhong Agricultural University
Chuang Wang
Huazhong Agricultural University
Lei Shi
Huazhong Agricultural University
Fangsen Xu (fangsenxu@mail.hzau.edu.cn)
Huazhong Agricultural University https://orcid.org/0000-0003-3564-1644

Research Article

Keywords: Brassica napus, BnaC4.BOR1;1c, boron response, boron acquisition

Posted Date: April 6th, 2021

DOI: https://doi.org/10.21203/rs.3.rs-385679/v1

Abstract

Aims

BnaC4.BOR1;1c is required for B acquisition in *Brassica napus* (*B. napus*) under low B stress. This study aimed to reveal the B regulatory mechanism of *BnaC4.BOR1;1c* and its physiological roles in B translocation from roots to shoots and B distribution in shoots.

Methods

Transgenic *Arabidopsis* plants expressing GUS (β-glucuronidase) under different promoters were generated and the mRNA, and GUS activity was quantitatively measured. The in-situ PCR and immunohistochemistry in *B. napus* were performed to investigate *BnaC4.BOR1;1c* expression pattern and localization. Furthermore, assays of B transport and distribution in wild type *B. napus* and *BnaC4.BOR1;1c* RNAi lines were carried out to elucidate its physiological roles.

Results

Results showed that *BnaC4.BOR1;1c* mRNA abundance is negatively correlated with B availability, which was mediated by the 29 nt sequence in the 5’ terminal region of 5’-UTR. Besides, the 5’-UTR simultaneously regulates protein expression level, most probably depending on the translation efficiency. BnaC4.BOR1;1c mainly localizes on the plasma membrane of vascular bundle cells in roots and shoots with a polar localization manner that is probably beneficial to B xylem loading in roots and B unloading from xylem to phloem in vascular bundle of shoots. Short-term ^{10}B uptake analysis demonstrates that *BnaC4.BOR1;1c* preferentially distributes B to developing leaves and flowers under B deficiency.

Conclusion

This study reveals combined regulatory action of mRNA abundance and translation efficiency mediated by the 5’-UTR in *BnaC4.BOR1;1c* in response to B availability and its physiological role in preferential B acquisition in developing tissues of *B. napus*.

Introduction

Boron (B) is one of the essential micronutrients for plant growth, but B excess is toxic. B plays an essential structural role in maintaining the cell wall integrity by crosslinking two rhamnogalacturonan II (RG-II) molecules to form RG-II-B complexes (O’Neill et al., 2001; Funakawa and Miwa, 2015). B is relatively immobile in plant cells; thus, B deficiency defects are early occurred in the developing tissues, such as necrosis and elongation cessation of the root tip, curl and reduced expansion of young leaves, and low fertility (Broadley et al., 2012; Zhang et al., 2017). Boron deficiency is a worldwide agricultural problem. The continuous B acquisition of plants from the environment mainly depends on two type B transporters. AtNIP5;1 (nodulin 26-like intrinsic protein 5;1) was identified as a boric acid influx transporter, and AtNIP5;1 protein mainly localizes on the plasma membrane (PM) toward the soil-side in

the outmost cell layer and endodermis of a root tip in *Arabidopsis* (Takano et al., 2006, 2010). Loss of *AtNIP5;1* function significantly reduces root B uptake capacity (Takano et al., 2006). *At*BOR1 functions as a boric acid/borate exporter on the PM of root epidermis and endodermis although expression in the cotyledon tip also reported (Takano et al., 2002; Yoshinari et al., 2016). In contrast to AtNIP5;1, AtBOR1 localizes on the PM toward the stele-side (Takano et al., 2010). Furthermore, many homologs of *Arabidopsis NIP5;1* and *BOR1* have been functionally characterized in succession in various species such as rice (Nakagawa et al., 2007; Hanaoka et al., 2014; Shao et al., 2021), barley (Sutton et al., 2007), wheat (Leaungthitikanchana et al., 2013), maize (Chatterjee et al., 2014; Durbak et al., 2014; Leonard et al., 2014) and oilseed rape (Zhang et al., 2017).

Efficient acquisition and avoiding B toxicity need a fine-tuning of the B homeostasis due to the narrow window of physiological B concentration between deficiency and toxicity (Warington, 1923; Nable et al., 1997). B concentration in vivo is negatively correlated with *AtNIP5;1* mRNA abundance in *Arabidopsis* through an AUG-stop element-mediated mRNA degradation procedure (Tanaka et al., 2011, 2016). In barley, reduced mRNA abundance of *HvNIP2;1* restricts B uptake leading to B toxicity tolerance in plants (Schnurbusch et al., 2010). The distinct B-dependent regulatory mechanisms are found in the *AtBOR1* gene expression regulation (Takano et al., 2010; Aibara et al., 2018). Protein translation efficiency of *AtBOR1* is inhibited upon the 5'-UTR, and its protein suffers degradation in the vacuole under high B stress (Kasai et al., 2011; Takano et al., 2010; Aibara et al., 2018). Besides, overexpression of *AtBOR4* (paralog of *AtBOR1*) can exclude B from the root resulting in enhanced tolerance to B toxicity (Miwa et al., 2007). A similar role of *Bot1* (*AtBOR1* homolog) in barley was characterized, and a high copy number of *Bot1* increases barley tolerance to B toxicity (Reid 2007; Sutton et al., 2007).

Developing tissue with low transpiration preferentially acquires B from xylem sap in many plants suggesting that B transporter might contribute to B translocation (Marentes et al., 1997; Huang et al., 2001; Takano et al., 2001; Matoh and Ochiai, 2005;). To date, *AtNIP6;1* and *AtNIP7;1* were functionally characterized to facilitate B acquisition in young leaves and flowers (Tanaka et al., 2008; Li et al., 2011; Routray et al., 2018). In rice, *OsNIP3;1* acts as a boric acid channel and preferentially distributes B to the developing tissues by unloading B from the xylem in nodes (Hanaoka et al., 2014; Shao et al., 2017). Besides, mineral element distribution in shoot tissues mediated by their transporters in the nodes has been well established in rice (Yamaji and Ma, 2014; 2017). However, little is known about the exact role of members of the BORs family in distributing B in shoots. We previously identified a boric acid/borate transporter gene *BnaC4.BOR1;1c* in *Brassica napus* (*B. napus*) with low B inducible expression pattern (Sun et al., 2012). *BnaC4.BOR1;1c* localizes in the stele of root, nodes in shoots, and base of the floral organ (Zhang et al., 2017). RNA interference of *BnaC4.BOR1;1c* significantly reduced B concentrations in shoots and flowers accompanied by the B defective phenotype of *B. napus* (Zhang et al., 2017), probably due to the reduced B xylem loading in roots. However, the B-dependent regulatory mechanism of *BnaC4.BOR1;1c* and its physiological role in B distribution in shoot tissues remains unclear. Here, we found that B not only regulates mRNA abundance but also adjusts BnaC4.BOR1;1c protein level in a 5'-UTR-dependent manner. Furthermore, tracer B experiments indicate that BnaC4.BOR1;1c plays a vital role

in preferentially distributing B from xylem to phloem in nodes for developing tissue growth under B deficiency.

Results

The 5′-UTR is required for the B-dependent regulation of BnaC4.BOR1;1c

It has been reported that low B upregulates *BnaC4.BOR1;1c* expression in a B-efficient *B. napus cv*. 'QY10' (Sun et al., 2012). To investigate the mechanism of B-dependent mRNA regulation, the mRNA abundance in *B. napus* root was quantified by quantitative real-time PCR (qRT-PCR) in the presence of low B (0.25 μM), medium B (25 μM), and high B (250 μM). Low B enhanced *BnaC4.BOR1;1c* expression relative to medium B condition, while high B significantly inhibited mRNA accumulation compared to medium B condition (Fig. 1a). This regulation pattern of *BnaC4.BOR1;1c* by B supply is similar to the B-dependent mRNA regulatory mechanism of *NIP5;1* in *Arabidopsis* (Tanaka et al., 2011, 2016). The 5′-UTR sequence of *BnaC4.BOR1;1c* was identified experimentally (Sun et al., 2012). We, therefore, generated transgenic *Arabidopsis* carrying the *ProBOR1;1c* (5′-UTR): GUS and 5′-UTR-deleted *ProBOR1;1c* (Δ5′-UTR): GUS to evaluate their effects on the expression abundance (Fig. 1b). The relative expression level of *GUS* in plants grown on 0.25 μM B or 250 μM B was determined. High B treatment accumulated lower *GUS* mRNA abundance relative to low B treatment in plants carrying *ProBOR1;1c* (5′-UTR): GUS construct (Fig. 1c). Construct with deletion of 5′-UTR was almost entirely insensitive to B regulation (Fig. 1c). These results demonstrate that 5′-UTR of *BnaC4.BOR1;1c* is required for the B-dependent mRNA abundance regulation.

5′ terminal region of 5′-UTR contributes to the B-dependent regulation of BnaC4.BOR1;1c

The 5′-UTR sequence of *BnaC4.BOR1;1c* consists of 351 nt upstream of its main open reading frame (ORF), in which two mini uORFs (Fig. 2a) and three more uORFs existed (Figure S1). Considering the important role of mini uORF and its upstream sequence in B-dependent mRNA regulation (Tanaka et al., 2011, 2016), the constructs of *Pro35S* (5′-UTR): GUS, *Pro35S* (5′-UTRΔ$^{1-29}$): GUS and *Pro35S* (5′-UTRΔ$^{1-97}$): GUS were generated to investigate the B response in *Arabidopsis* plants (Fig. 2). The 29 nt region and 97 nt region in the 5′ terminal region includes the first AUG-stop and second AUG-stop, respectively (Fig. 2a and Figure S1). Either 1–29 nt deletion or 1–97 nt deletion from the 5′ terminal region in the 5′-UTR completely abolished the high B effect on the mRNA (Fig. 2c), suggesting that the 29 nt sequence in the 5′ terminal region of 5′-UTR is required for the high B response. We further validated this conclusion that deletion of 92–97 nt (corresponding to second AUG-stop, Fig. 2a) in the 5′-UTR maintained a rapid high B response (Fig. 2c). Consistent with this, both 1–29 nt deletion and 1–97 nt deletion significantly reduced the high B inhibition of GUS activity relative to low B condition, and the relative GUS activity of deletion of the 92–97 nt in the 5′-UTR remained lower level at high B condition (Figure S2). Interestingly, compared with low B condition, the GUS activities of *Pro35S*:(5′- UTRΔ$^{1-29}$): GUS and *Pro35S*:(5′-UTRΔ$^{1-97}$): GUS were partially reduced at high B condition (Figure S2), though their mRNA levels were

comparable at both low B and high B conditions (Fig. 2c). Taken together, these results suggest that the 5’ terminal 1–29 nt region in the 5’-UTR contributes to the B-dependent regulation of *BnaC4.BOR1;1c*.

Localization of BnaC4.BOR1;1c in B. napus

Undoubtedly, the total reduced B content in the shoots of BnaC4.BOR1;1c RNAi plants can be ascribed to the down translocation of B in the roots of *BnaC4.BOR1;1c* (Zhang et al., 2017). Although *BnaC4.BOR1;1c* promoter activity has been observed in the root stele, node, and base of the floral organ in pro*BnaC4.BOR1;1c: GUS* transgenic *Arabidopsis* (Zhang et al., 2017), the details of BnaC4.BOR1;1c localization in these tissues of *B. napus* is not clarified. To this end, we first performed the in-situ PCR (Athman et al., 2014) of *BnaC4.BOR1;1c* in the root, hypocotyl, and node of *B. napus*. For the negative control, no *BnaC4.BOR1;1c* reverse primer was used in the reverse transcription PCR. Compared with negative control (Fig. 3a), a strong signal was detected in the cells surrounding the stele of root (Fig. 3b). In the hypocotyl, the signal mainly existed in the vascular tissues (Fig. 3d, e), while no detectable signal was showed in the negative control (Fig. 3c). Then the localization of *BnaC4.BOR1;1c* mRNA in the nodes was investigated. The vascular bundles showed clear signals (Fig. 3f), including the xylem, cambium (Fig. 3h), and indeed no specific signal was detected in these cells of negative control (Fig. 3g).

In parallel, we performed immunohistochemistry staining of the roots and nodes of *B. napus* using an antibody that was generated against an artificial peptide of the BnaC4.BOR1;1c region (SSTPLNNRSLSSPR). The plants ‘QY10’ and RNAi plants grown on 0.25 μM B were sampled for the positive and negative control, respectively. The strong green signal was imaged on the PM of cells surrounding stele in ‘QY’ roots (Fig. 4a, b) compared to the RNAi plants (Fig. 4c, d). In line with the polar localization of AtBOR1 on the PM of root cells toward the stele-side (Takano et al., 2010), the polar localization toward the stele-side was observed in *B. napus* (Fig. 4a, b). In the nodes of *B. napus*, the signal was mainly detected in the xylem and cambium of vascular bundles (Fig. 4e-h). Polar localization on the cambium cell toward to phloem was observed. Furthermore, 250 μM B is sufficient to abolish BnaC4.BOR1;1c protein accumulation in roots and nodes (Fig. 4i-l). Because the artificial peptide of BnaC4.BOR1;1c was partially conserved among BnaBOR1s (Figure S3), the results presumably represent the localization of multiple BnaBOR1 proteins in *B. napus*. To clarify the localization of BnaC4.BOR1;1c, transgenic Arabidopsis expressing BnaC4.BOR1;1c-GFP was generated. Polar localization of BnaC4.BOR1;1c-GFP toward stele-side on the PM of both epidermis and endodermis was observed in *Arabidopsis* (Fig. 4m-o). Taken together, these results demonstrate that BnaC4.BOR1;1c is polarly localized on the PM of cells in vascular tissues.

BnaC4.BOR1;1c transports B in yeast and in B. napus

Despite the symptoms of B deficiency were observed in *BnaC4.BOR1;1c* RNAi *B. napus* (Zhang et al., 2017), the transport activity of BnaC4.BOR1;1c is not validated in the plant. Previously, the B transport activity of BnaC4.BOR1;1c in yeast was reported (Diehn et al., 2019), while yeast expressing BnaC4.BOR1;1c did not show stronger growth than that of yeast expressing empty vector on the high B medium (Diehn et al., 2019). To clarify the B transport activity of BnaC4.BOR1;1c, yeast *Scbor1* mutant

was employed to express target genes. AtBOR1 was used as a positive control because its B transport activity had been demonstrated (Takano et al., 2002). In agreement with the result (Diehn et al., 2019), the yeasts with induction of pYES2, AtBOR1, and BnaC4.BOR1;1c did not show distinct growth inhibition on the medium without B, while the best growth was observed for the AtBOR1-yeast, then followed by BnaC4.BOR1;1c-yeast, and the pYES2-yeast at the 20 mM B medium (Figure S4). The similar growth between pYES2-yeast and BnaC4.BOR1;1c yeast cannot strongly demonstrate that BnaC4.BOR1;1c can export B from yeast cells. Thus, we further compared the intracellular B concentrations among these yeasts. Yeasts were incubated in 500 μM B for 60 min in galactose medium, the pYES2-yeast had about 1.1 mmol B/ kg DW, while both AtBOR1-yeast and BnaC4.BOR1;1-yeast had lower B concentrations (~ 0.34 mmol B/kg DW and ~ 0.52 mmol B/kg DW) (Fig. 5a). This result demonstrated that BnaC4.BOR1;1c has B transport activity. The B transport activity of BnaC4.BOR1;1c was further investigated in *B. napus* using the RNAi lines for B's transient uptake assay (Zhang et al., 2017). Plants grown hydroponically with 100 μM ^{11}B were transferred to 0.25 μM ^{11}B for 24 h, then 5 μM ^{10}B for 24 h, and the ^{10}B concentrations in roots and shoots were measured by inductively coupled plasma-mass spectrometry (ICP-MS). The amount of ^{10}B transported into shoots per unit dry weight of roots within 24 h was defined as the BnaC4.BOR1;1c function in roots. The RNAi lines showed lower ^{10}B accumulation in shoots than wild-type 'QY10' (Fig. 5b), indicating that BnaC4.BOR1;1c can facilitate B translocation from roots into shoots.

BnaC4.BOR1;1c contributes to preferential B acquisition of developing tissues under B deficiency

To investigate whether BnaC4.BOR1;1c contributes to B acquisition in developing tissues in shoots such as flower and young leaves; labeling experiments were performed using the isotope B. The top inflorescence of wild-type 'QY10' and *BnaC4.BOR1;1c* RNAi lines grown in ^{11}B-enriched solution (100 μM) were incubated in 5 μM ^{10}B-enriched solution for two days. ICP-MS measurement of ^{10}B concentration showed that wild-type buds had higher B concentrations than RNAi buds (Fig. 6a). This result indicates that BnaC4.BOR1;1c contributes to B acquisition of buds. B is usually immobile in most plant species (Brown and Shelp, 1997). We tested the B mobility in *B. napus* and the potential role of BnaC4.BOR1;1c in this process using RNAi lines. Seedlings grown in ^{11}B-enriched solution (100 μM) were transferred to 0 μM B for two days. B concentration was reduced in the new leaves and old leaves (Fig. 6b). No obvious reduction was observed in other tissues. The distribution ratio of B in new leaves was increased after B starvation, while it was decreased in old leaves (Fig. 6c). No big changes were detected for other tissues. Although a small amount of B was transported into new leaves from other tissues, the distribution pattern among wild-type plants and RNAi lines was similar, suggesting that *BnaC4.BOR1;1c* did not contribute to this process. To clarify whether *BnaC4.BOR1;1c* is involved in preferential B translocation into new leaves; we performed the transient B uptake assay of *B. napus* seedlings. To avoid the B transport activity of BnaC4.BOR1;1c in roots, chimera *B. napus* plants were generated (Fig. 6d) by grafting the wild type and RNAi scions on the wild-type rootstocks (named graft^{WT} and graft^{Ri}). Chimera plant grown in the ^{11}B-enriched solution was transferred to 0.1 μM ^{11}B-enriched medium for one day followed by two days exposure in 1 μM ^{10}B. The ^{10}B concentrations in young leaves (L1) of graft^{Ri} was lower than that in graft^{WT} (Fig. 6e). In contrast, ^{10}B concentration in hypocotyls of graft^{Ri} was higher than that in grafts^{WT}

(Fig. 6e). In parallel, the distribution ratio of B was lower for graft^{Ri} young leaves (L1) and higher for graft^{Ri} stems and hypocotyls relative to that of graft^{WT} (Fig. 6f). These results demonstrate that BnaC4.BOR1;1c facilitates the preferential distribution of B into developing tissues such as buds and leaves.

Discussion

Increasing studies had reported that vascular localization of various transporters in the shoots play an essential role in their substrate's mobility, such as NIP6;1 for the B acquisition of young leaves in *Arabidopsis* (Tanaka et al., 2008) and OsNIP3;1 for the B distribution into leaves in rice (Shao et al., 2017).

BnaC4.BOR1;1c **is regulated in response to B availability mediated by 5'-UTR**

B homeostasis is essential for the optimal growth of the plant through fine-tuning B transporter expression. In China, a large agricultural soil area of usually possesses low B concentrations, which cannot satisfy the growing demand of *B. napus* (Xu et al., 2001). *BnaC4.BOR1;1c* was up-regulated by low B in the root, shoot, and flower of *B. napus* 'QY10' (Sun et al., 2012), and its expression level increased gradually within 24 h of low B treatment (Chen et al., 2018). Low B inducible expression of *BnaC4.BOR1;1c* probably contributes to the B efficiency in 'QY10'. However, the low sensitivity of *BnaC4.BOR1;1c* to low B stress was reported in a European winter-type *B. napus cv.* Darmor-PBY018 (Diehn et al., 2019). Therefore, different *B. napus cv*. might have distinct B response of *BnaC4.BOR1;1c*.

In this study, we demonstrate that the 5' terminal 29 nt in the 5'-UTR of *BnaC4.BOR1;1c* of 'QY10' mediates the B response (Fig. 1 and Fig. 2). In *Arabidopsis*, the transcription level of *AtNIP5;1* was down-regulated by high B (Takano et al., 2006), and the 5'-UTR of *AtNIP5;1* is required for B-dependent mRNA degradation (Tanaka et al., 2011). Furthermore, the 'AUGUAA' cis-element in the 5'-UTR and its upstream conserved sequence 'UAUA' were found to induce ribosome stalling and mRNA degradation under high B conditions (Tanaka et al., 2016). Interestingly, the 29 nt in the 5'-UTR of *BnaC4.BOR1;1c* includes a mini uORF (AUGUAA) and, in particular, a sequence consensus 'CAUA' at the same position (Figure S1) corresponding to the 'UAUA' in 5'-UTR of AtNIP5;1. These results suggest that a common mechanism of B-dependent mRNA regulation might exist in both *AtNIP5;1* and *BnaC4.BOR1;1c* in 'QY10'. However, the high B response of *AtNIP5;1* is stronger (Takano et al., 2006) than that of *BnaC4.BOR1;1c*, probably due to the sequence inconsistency between them. 'ZS11' is a conventional commercial cultivar with high B efficiency in China (Hua et al., 2016). We compared their 5'-UTR sequences of *BnaC4.BOR1;1c* (Figure S5) and found significant differences existed in the region between uORF1 and uORF2. Most importantly, mRNA degradation associated upstream conserved sequence before uORF ('UAUA' in *AtNIP5;1* and 'CAUA' in 'QY10' *BnaC4.BOR1;1c*) was '-ACA' in 'ZS11' (Figure S5). This result implies that *BnaC4.BOR1;1c* might have different B responses among *B. napus* lines

On the other hand, AtBOR1 showed two B-dependent regulatory mechanisms, in which high B rapidly triggers BOR1 protein endocytosis from PM for degradation in the vacuole (Takano et al., 2005, 2010; Kasai et al., 2011), and continuous toxic B supply induces translational suppression in the 5′-UTR (Aibara et al., 2018). The high B-dependent translational suppression in the 5′-UTR of *AtBOR1* was mediated by the multiple uORFs (Aibara et al., 2018). B-dependent regulation of *AtNIP5;1* together *AtBOR1* cooperatively maintain B homeostasis. We found a total of 5 uORFs in the 5′-UTR of *BnaC4.BOR1;1c* (Figure S1). Despite the deletion of 29 nt or 97 nt abolished the high B effect on mRNA abundance, the protein level was reduced partially under high B treatment (Figure S2). One possibility is that high B inhibits protein translation efficiency through 5′-UTR of *BnaC4.BOR1;1c*. The sequences uORF3, uORF4 and uORF5 in 5′-UTR of *BnaC4.BOR1;1c* between 'QY10' and 'ZS11' possess high conservation (Figure S5), suggesting B-dependent protein translation regulation of BnaC4.BOR1;1 gene is generalized for *B. napus*. Together, these results revealed a combined regulatory action of mRNA abundance and translation efficiency mediated by the 5′-UTR of 'QY10' *BnaC4.BOR1;1c* in response to B availability.

BnaC4.BOR1;1c is responsible for B loading in roots and preferential distribution of B to developing tissues in shoots

It is conceivable that BnaC4.BOR1;1c may have common characteristics as AtBOR1 because of the high similarity of protein sequences such as polar localization of BnaC4.BOR1;1c on the PM of root cells toward the stele-side (Fig. 4). This polar localization presumably contributes to efficient B loading into the xylem in roots.

In *Arabidopsis*, polar localization of AtBOR1 localizes on the PM of epidermis and endodermis toward the stele-side in roots was proposed to efficiently load B into xylem for translocation (Takano et al., 2008). The B transport activity assays of BnaC4.BOR1;1c in yeast and *B. napus* directly support that BnaC4.BOR1;1c is responsible for B loading in the root (Fig. 5).

Developing tissue in the shoot has low or no transpiration capability; thus the mineral elements demand is proposed to be facilitated preferentially by various transporters. The connection sites such as node and base of floral organ linking developing tissues and stem are important hubs for the nutrient's distribution (Yamaji and Ma, 2014). In *Arabidopsis*, *AtBOR1* contributes to the preferential translocation of B to young leaves, while it is unclear that whether *AtBOR1* functions at such hubs (Takano et al., 2001) because no evidence of AtBOR1in nodes was documented. The xylem-to-phloem transfer of B is mediated by the *AtNIP6;1* in *Arabidopsis* (Tanaka et al., 2008) and by the *OsNIP3;1* in rice (Shao et al., 2017) under low B conditions since their specific localization in the vascular cells. Most recently, rice OsBOR1 was found to be polarly localized in bundle sheath cells of nodes and xylem parenchyma cells of the leaf sheath, and it plays a vital role in distributing B to new leaves and panicles (Shao et al., 2021). In this study, we found that *BnaC4.BOR1;1c* is localized in the vascular xylem and cambium cells region in the nodes of developing tissues (Fig. 3), distinct from the AtBOR1 localization in the shoot (Yoshinari et al., 2016), implying the different roles between AtBOR1 and BnaC4.BOR1;1c. The biomass of *B. napus* is far more than the biomass of *Arabidopsis*; thus the efficient B acquisition is necessary to sustain optimal growth.

There is little doubt that the vascular localization of BnaC4.BOR1;1c might contribute to B re-distribution or distribution in shoot tissues. B is usually immobile in most plant species (Brown and Shelp, 1997). Based on our experiments, BnaC4.BOR1;1c did not contribute to the B re-distribution in shoots (Fig. 6b, c), although a small proportion B was redistributed into young leaves (Fig. 6c) when plants were transferred from adequate B condition to B starvation condition, probably due to free B in plants. The tracer analyses of B uptake in *B. napus* buds (Fig. 6a) and in grafted plants (Fig. 6d-f) demonstrated that BnaC4.BOR1;1c is important for the preferential distribution of B in developing tissues. These results suggest that BOR1 protein plays a similar role in *B. napus* and rice. Furthermore, we observed the polar localization of BnaBOR1s, including BnaC4.BOR1;1c on the PM of cambium cells toward phloem (Fig. 4e-h). A reasonable answer to this is that polar localization of BnaBOR1s in cambium cells is beneficial to B translocation from the xylem into the phloem. Taken together, the present data reveal that BnaC4.BOR1;1c is responsible for B loading in root and preferential distribution of B to developing tissues.

Materials And Methods

Plant materials and growth conditions

B-efficient *B. napus* 'QY10' (winter-type *B. napus* in China), the RNAi lines of *BnaC4.BOR1;1c* (Zhang et al., 2017), transgenic *Arabidopsis* (Col-0 background) were used in this study. For the pot growth of *B. napus*, seeds were sown in the soil, which includes 0.85 g NH_4NO_3 kg^{-1}, 383.3 mg $KH_2PO_4{\cdot}2H_2O$ kg^{-1}, 250 mg $MgSO_4{\cdot}7H_2O$ kg^{-1}, 751.1 mg KCl kg^{-1}. Pots were irrigated with 1,500 ml ultrapure water supplemented with micronutrients (3.5 mg ^{11}B, 12.60 mg $MnCl_2{\cdot}4H_2O$, 1.54 mg $ZnSO_4{\cdot}7H_2O$, 0.56 mg $CuSO_4{\cdot}5H_2O$, 0.168 mg $Na_2MoO_4{\cdot}2H_2O$, 1.75 mmol Fe-EDTA) to maintain proper humidity. For the inflorescence tracer B experiment, the inflorescences with stem segments about 15 cm in length were cut and cultured two days in a hydroponic box with 5 μM ^{10}B. For the hydroponic growth of *B. napus*, seeds were surface-sterilized. They germinated one week in ultrapure water and then were transferred into a quarter-strength solution for 5 days growth followed by 5 days half-strength solution treatment and full-strength solution culture. Modified Hoagland's solution was used in hydroponic growth (Li et al., 2019), in which 100 μM ^{11}B was used. For the tracer B experiment of seedlings, seedlings of *B. napus* were washed with ultrapure water and then treated in 0.25 μM ^{11}B for 1 day followed by one-day growth in 5 μM ^{10}B. For the *Arabidopsis* culture, a solid MGRL medium was prepared (Fujiwara et al., 1992) with 1% gellan gum and 1% sucrose. Transgenic Arabidopsis lines were established by the *Agrobacterium*-mediated in planta method (Clough and Bent, 1998). To generate chimera *B. napus* plants, a scion cut at 1-2 cm under cotyledon was inserted into a rootstock at the position 1 cm above the cotyledon. A silicon tube was used to support vertical growth. The grafted plants were placed in a transparent box with very high artificial humility. After one-week, grafted plants were successfully established.

Plasmid construction

To construct *ProBOR1;1c* (5'-UTR): GUS and *ProBOR1;1c* (Δ5'-UTR): GUS, promoter sequences of *BnaC4.BOR1;1c* with or without 5'-UTR were amplified from 'QY10' DNA by PCR reaction with specific primers (Table S1), then fused with *Sca*I and *Sma*I digested PBI121 fragment using In-Fusion Cloning kits (Clontech). To construct *Pro35S* 5'UTR: GUS, *Pro35S* 5'UTR$^{\Delta 1\text{-}29}$: GUS, and *Pro35S* 5'UTR$^{\Delta 1\text{-}97}$: GUS, truncated 5' UTR sequences were amplified by PCR reaction with specific primers (Table S1) and were fused with XbaI digested PBI121using In-Fusion Cloning kits (Clontech). To generate *Pro35S* 5'UTR$^{\Delta 1\text{-}29}$: GUS, *Pro35S* 5'UTR: GUS was used as a template by PCR reaction using specific primers, and the PCR product was self-fused.

Gene expression analysis

To investigate *GUS* expression, 10-d-old *Arabidopsis* seedlings grown on 100 μM B were transferred to 0.25 μM B or 250 μM B medium for 2 d growth. Plants were harvested for sampling. RNA was extracted using TRIZOL Reagent (Invitrogen, CA, USA). Reverse transcription was carried out using M-MLVReverse Transcriptase (Promega) according to the manufacturer's protocol. RT fluorescence quantitative PCR was performed using the SYBR Green Real-Time PCR Master Mix Kit (Toyobo, Japan) and the CFX96^{TM} Real-Time PCR Detection System (Bio-Rad, Hercules, CA, USA). Actin and Tubulin were used as internal controls with primers F: 5'-ACAGTGTCTGGATCGGTGGTTC-3', R: 5'-TGCCTCATCATACTCAGCCTTG-3' (ACTIN); F: 5'-CAGCAATACAGTGCCTTGAGTG-3', R: 5'-CCTGTGTACCAATGAAGGAAAGCC-3' (TUBULIN). Each gene's relative expression level was calculated and normalized based on these two internal controls using the ΔΔCt method (Livak & Schmittgen 2001).

β-Glucuronidase (GUS) histochemical staining and quantification of GUS activity

β-Glucuronidase (GUS) histochemical staining of *GUS* reporter lines was performed using the GUS Histochemical Kit (bioshap, Cat. BL622A). The sample photos were taken using an Olympus SZX16 stereomicroscope. For the GUS activity assay, GUS line's total protein was extracted using the GUS extraction buffer (50 mM sodium phosphate buffer (pH 7.0), 10 mM β-mercaptoethanol, 1 mM Na_2-EDTA·$2H_2O$, and 0.1% Triton X-100). After centrifugation at 12,000 rpm, the total protein concentration was determined by using the Bradford assay (Bradford, 1976). 50 μg of total protein was mixed with 450 μL MUG buffer incubated at 37°C. 40 μL interaction solution was obtained at 5 min, 15, 25, or 35 min, respectively, and mixed with 160 μL of 0.2 M Na_2CO_3 to stop the interaction. GUS fluorescence (excitation: 365 nm; emission: 455 nm) was measured using a microplate reader (TECAN Infinite M200). The standard curve was established by mixing 40 μL 4-MU (4-methylumbelliferone) and 160 μL 0.2 M Na_2CO_3, in which the 4-MU was set as $1/2^6$ mM, $1/2^7$ mM, until to$1/2^{12}$ mM).

Immunohistological staining of BnaC4.BOR1;1c

To perform in vivo immunohistological staining of BnaC4.BOR1;1c in *B. napus*, an antibody against BnaC4.BOR1;1c was obtained by purifying the rabbit antiserum, which was prepared through immunizing rabbits with an artificial peptide (SSTPLNNRSLSSPR). The immunohistological staining method (Ma et

al., 2007) was used with modification. Briefly, *B. napus* seedlings (20-d-old), precultured in 25 μM B, were transferred to 0.25 μM B or 250 μM B for 2 d growth. The roots, basal node, and nodes (petiole junction) from 'QY10' and RNAi plants were cut as ~0.5-1 cm thickness and fixed in the solution at 4 ℃ (4% paraformaldehyde, 60 mM sucrose, and 50 mM Cacodylic acid). The samples were centrifuged at 7,000 rpm for 2 min. After exposed to room temperature for 2 h, samples were washed several times using 1 x PBS buffer, then embedded by 5% agar (Nakalai, Tesque, Kyoto, Japan) for solid at 4℃. 100 μm specimens were prepared using a semi-automatic slicer and stored in 1xPBS buffer. Then the specimens were incubated in the 1xPBS buffer supplemented with 0.1%(w/v) pectolyase+0.3%(w/v) Triton X-100 for 2 h. After washed with 1xPBS, the specimens were blocked in 5% (w/v) BSA/PBS for 10 min, followed incubated with primary antibody (anti-BnaC4.BOR1;1c, rabbit, 1:1000 dilution) for overnight. After washed with 1xPBS buffer, the specimens were incubated in secondary antibody (Alexa fluor 488-conjugated Goat anti-rabbit IgG (H+L) AS053, 1:2000 dilution) for 2 h without light. The specimens were then washed 5 times in 1 x PBS and mounted with an antifade polyvinylpyrrolidone mounting medium (Beyotime, Shanghai, China). Fluorescence imaging was examined in the Leica SP8 system (Leica, Mannheim, Germany). GFP was excited by 488 nm, and the signal was collected from 505-545 nm wavelength.

In situ PCR

The *in situ* PCR method (Athman et al., 2014) was used with modification. Briefly, fresh plant tissues were fixed overnight in FAA solution (63% ethanol, 5% acetic acid, and 2% formalin) without vacuum infiltration step. After three times washes by buffer (63% ethanol and 5% acetic acid) and one-time wash by 1xPBS buffer, the samples were embedded in 5% agar (Nakalai, Tesque, Kyoto, Japan) for solid at 4 ℃. 75 μm specimens were prepared using a semi-automatic slicer and stored in DEPC water containing 100 U RNaseOUT (Takara Bio, Japan), 2.5% DNase I (Promega, China) followed by 45 min incubation at 37ºC. Then 15 mM EDTA was used to stop the reaction at 70ºC for 15 min. After wash by cold DEPC water, the reverse transcription (Promega, China) was performed in the RT mix with *BnaC4.BOR1;1c* specific primer (4 μl 5 X buffer, 2 μl 10 mM dNTPs, 1 μl 0.1 M DTT, 10 μl H_2O and 1 μl reverse primer at 65ºC for 5 min. Then 1 μl M-MLVReverse Transcriptase and 1 μl RNaseOUT were added into the tube on the ice, followed by 1 h incubation at 50ºC and 5 min at 85ºC. The negative control was prepared as above without a specific primer. Specimens were transferred into tube containing PCR mix [5 μl 10 x Taq buffer (Aidlab bio.), 1 μl 10 mM mixed dNTPs , 0.2 μl digoxigenin-11-dUTP (Roche; 4 μM), 2.5 μl 10 mM forward primer, 2.5 μl 10 mM reverse primer, 1 μl Taq polymerase (Aidlab bio), 38.3 μl H_2O]. After twice washes by 1 x PBS, specimens were blocked 30 min in 1 x block solution at room temperature (10 mg BSA in 10 ml 1 x PBS). 1.5 U AP-conjugated anti-DIG Fab fragments (Roche) were added for 1 h incubation at room temperature. The specimens were washed twice for 15 min using buffer (0.1 M Tris-Cl; 0.15 M NaCl, pH 9.5) and then incubated in 50 μl BM purple (Roche) for 2 h. Twice washes by washing buffer to remove the blue solution, the specimens were mounted on the microscope slide for imaging.

Measurement of B concentration

All samples were dried at 65°C in an oven for 3-4 d and then ground into fine powders using carnelian mortar. 1 M HCl was used to digest dry powders on the shaker for 2 h at 250 rpm. The solution was filtered, and B concentration was measured by inductively coupled plasma mass spectrometer (ELAN DRC-e; Perkin Elmer, USA).

Statistical Analysis of Data

Data were analyzed using Student's *t*-test and Duncan's test. Significance was defined when P value < 0.05.

Declarations

Acknowledgements

This work was funded by the National Key Research and Development Program of China (Grant no. 2016YFD0100700), National Natural Science Foundation of China (Grant no. 31772380), the Fundamental Research Funds for the Central Universities of China (Grant No. 2662019PY058, 2662019PY013), and Natural Science Foundation of Hubei Province (2019CFB467). We thank Dr. Limei Zhang and Xiangsheng Ye (Huazhong Agricultural University, China) for the technical assistance.

Conflict of interest

The authors declare no competing financial interests.

Author contributions

F.X. and S.W designed the research; S.W, L.L, D.Z, Y.H and Z.Z performed the experiments and analyzed the data; S.W. wrote the manuscript; all authors read and approved it.

References

1. Aibara I, Hirai T, Kasai K, Takano J, Onouchi H, Naito S, Fujiwara T, Miwa, K (2018)Boron-dependent translational suppression of the borate exporter BOR1 contributes to the avoidance of boron toxicity. Plant Physiol 177:759–774
2. Athman A, Tanz SK, Conn VM, Jordans C, Mayo GM, Ng WW, Burton RA, Conn SJ, Gilliham M (2014) Protocol: A fast and simple in situ PCR method for localising gene expression in plant tissue. Plant Methods 10:29
3. Bradford MM (1976) A rapid and sensitive method for the quantitation of microgram quantities of protein utilizing the principle of protein-dye binding. Anal Biochem 72:248–254
4. Broadley M, Brown P, Cakmak I, Rengel Z, Zhao F (2012) Function of Nutrients: Micronutrients. In: Marschner's Mineral Nutrition of Higher Plants, 3rd edn. Academic Press, San Diego, pp 191–248
5. Brown PH, Shelp BJ (1997) Boron mobility in plants. Plant Soil 193:85–101

6. Chatterjee M, Tabi Z, Galli M, Malcomber S, Buck A, Muszynski M, Gallavotti A (2014) The boron efflux transporter ROTTEN EAR is required for maize inflorescence development and fertility. Plant Cell 26:1–17
7. Chen H, Zhang Q, He M, Wang S, Shi L, Xu F (2018) Molecular characterization of the genome-wide *BOR* transporter gene family and genetic analysis of *BnaC04.BOR1;1c* in *Brassica napus*. BMC Plant Biol 18:1–14
8. Clough SJ, Bent AF (1998) Floral dip: a simplified method for Agrobacterium-mediated transformation of *Arabidopsis thaliana*. Plant J 16:735–743
9. Diehn T A, Bienert M D, Pommerrenig B, Liu Z, Spitzer C, Bernhardt N, Fuge J, Bieber A, Richet N, Chaumont F, Bienert G P. (2019). Boron demanding tissues of Brassica napus express specific sets of functional Nodulin26-like Intrinsic Proteins and BOR1 transporters. Plant J 100: 68–82
10. Durbak AR, Phillips KA, Pike S, O'Neill MA, Mares J, Gallavotti A, Malcomber ST, Gassmann W, McSteen P (2014) Transport of boron by the tassel-less1 aquaporin is critical for vegetative and reproductive development in maize. Plant Cell 26:2978–2995
11. Fujiwara T, Hirai MY, Chino M, Komeda Y, Naito S (1992) Effects of sulfur nutrition on expression of the soybean seed storage protein genes in transgenic petunia. Plant Physiol 99:263–268
12. Funakawa H, Miwa K (2015) Synthesis of borate cross-linked rhamnogalacturonan II. Front Plant Sci 6:223
13. Hanaoka H, Uraguchi S, Takan J, Tanaka M, Fujiwara T (2014) OsNIP3;1, a rice boric acid channel, regulates boron distribution and is essential for growth under boron-deficient conditions. Plant J 78:890–902
14. Hua Y, Zhang D, Zhou T, He M, Ding G, Shi L, Xu F (2016) Transcriptomics-assisted quantitative trait locus fine mapping for the rapid identification of a nodulin 26-like intrinsic protein gene regulating boron efficiency in allotetraploid rapeseed. Plant, Cell Environ. 39: 1601–1618
15. Huang L, Bell RW, Dell B (2001) Boron supply into wheat (*Triticum aestivum L. cv. Wilgoyne*) ears whilst still enclosed within leaf sheaths. J Exp Bot 52:1731–1738
16. Kasai K, Takano J, Miwa K, Toyoda A, Fujiwara T (2011) High boron-induced ubiquitination regulates vacuolar sorting of the BOR1 borate transporter in *Arabidopsis thaliana*. J Biol Chem 286:6175–6183
17. Leaungthitikanchana S, Fujibe T, Tanaka M, Wang S, Sotta N, Takano J, Fujiwara T (2013)Differential expression of three *BOR1* genes corresponding to different genomes in response to boron conditions in hexaploid wheat (*Triticum aestivum L.*). Plant Cell Physiol 54:1056–1063
18. Leonard A, Holloway B, Guo M, Rupe M, Yu G, Beatty M, Zastrow-Hayes G, Meeley R, Llaca V, Butler K et al (2014) *tassel-less1* encodes a boron channel protein required for inflorescence development in maize. Plant Cell Physiol 55:1044–1054
19. Livak KJ, Schmittgen TD (2001) Analysis of relative gene expression data using real-time quantitative PCR and the 2-ΔΔCT method. Methods 25:402–408

20. Li T, Choi W-G, Wallace IS, Baudry J, Roberts DM (2011) Arabidopsis thaliana NIP7;1: an anther-specific boric acid transporter of the aquaporin superfamily regulated by an unusual tyrosine in helix 2 of the transport pore. Biochemistry 50:6633–6641
21. Li Y, Wang X, Zhang H, Wang S, Ye X, Shi L, Xu F, Ding G (2019) Molecular identification of the phosphate transporter family 1 (*PHT1*) genes and their expression profiles in response to phosphorus deprivation and other abiotic stresses in *Brassica napus*. PLoS One 14:1–23
22. Ma JF, Yamaji N, Mitani N, Tamai K, Konishi S, Fujiwara T, Katsuhara M, Yano M (2007) An efflux transporter of silicon in rice. Nature 448:209–212
23. Marentes E, Shelp BJ, Vanderpool RA, Spiers GA (1997) Retranslocation of boron in broccoli and lupin during early reproductive growth. Physiol Plant 100:389–399
24. Matoh T, Ochiai K (2005) Distribution and partitioning of newly taken-up boron in sunflower. Plant Soil 278:351–360
25. Miwa K, Takano J, Omori H, Seki M, Shinozaki K, Fujiwara T (2007) Plants tolerant of high boron levels. Science 318:1417
26. Nable RO, Bañuelos GS, Paull JG (1997) Boron toxicity. Plant Soil 193:181–198
27. O'Neill MA (2001) Requirement of borate cross-linking of cell wall rhamnogalacturonan II for *arabidopsis* growth. Science 294:846–849
28. Nakagawa Y, Hanaoka H, Kobayashi M, Miyoshi K, Miwa K, Fujiwara T (2007) Cell-type specificity of the expression of *Os BOR1*, a rice efflux boron transporter gene, is regulated in response to boron availability for efficient boron uptake and xylem loading. Plant Cell 19:2624–2635
29. Reid R (2007) Identification of boron transporter genes likely to be responsible for tolerance to boron toxicity in wheat and barley. Plant cell Physiol 48:1673–1678
30. Routray P, Li T, Yamasaki A, Yoshinari A, Takano J, Choi WG, Sams CE, Roberts DM (2018) Nodulin intrinsic protein 7;1 is a tapetal boric acid channel involved in pollen cell wall formation. Plant Physiol 178:1269–1283
31. Schnurbusch T, Hayes J, Hrmova M, Baumann U, Ramesh SA, Tyerman SD, Langridge P, Sutton T (2010) Boron toxicity tolerance in barley through reduced expression of the multifunctional aquaporin HvNIP2;1. Plant Physiol
32. Sun J, Shi L, Zhang C, Xu F (2012) Cloning and characterization of boron transporters in *Brassica napus*. Mol Biol Rep 39:1963–1973
33. Shao J, Yamaji N, Liu XW, Yokosho K, Shen RF, Ma JF (2018) Preferential distribution of boron to developing tissues is mediated by the intrinsic protein OsNIP3;1. Plant Physiol 176:1739–1750
34. Shao JF, Yamaji N, Huang S, Ma JF (2021) Fine regulation system for distribution of boron to different tissues in rice. New Phytol 230:656–668
35. Sutton T, Baumann U, Hayes J, Collins NC, Shi B-J, Schnurbusch T, Hay A, Mayo G, Pallotta M, Tester M et al (2007) Boron-toxicity tolerance in barley arising from efflux transporter amplification. Science 318:1446–1449

36. Takano J, Miwa K, Fujiwara T (2008) Boron transport mechanisms: collaboration of channels and transporters. Trends Plant Sci 13:451–457
37. Takano J, Miwa K, Yuan L, von Wirén N, Fujiwara T (2005) Endocytosis and degradation of BOR1, a boron transporter of *Arabidopsis thaliana*, regulated by boron availability. Proc Natl Acad Sci U S A 102:12276–12281
38. Takano J, Noguchi K, Yasumori M, Kobayashi M, Gajdos Z, Miwa K, Hayashi H, Yoneyama T, Fujiwara T (2002) Arabidopsis boron transporter for xylem loading. Nature 420:337–340
39. Takano J, Tanaka M, Toyoda A, Miwa K, Kasai K, Fuji K, Onouchi H, Naito S, Fujiwara T (2010) Polar localization and degradation of *Arabidopsis* boron transporters through distinct trafficking pathways. Proc Natl Acad Sci U S A 107:5220–5225
40. Takano J, Wada M, Ludewig U, Schaaf G, von Wirén N, Fujiwara T (2006) The *Arabidopsis* major intrinsic protein NIP5;1 is essential for efficient boron uptake and plant development under boron limitation. Plant Cell 18:1498–1509
41. Takano J, Yamagami M, Noguchi K, Hayashi H, Fujiwara T (2001) preferential translocation of boron to young leaves in *Arabidopsis thaliana* regulated by the *BOR1* gene. Soil Sci Plant Nutr 47:345–357
42. Tanaka M, Sotta N, Yamazumi Y, Yamashita Y, Miwa K, Murota K, Chiba Y, Hirai MY, Akiyama T, Onouchi H et al (2016) The minimum open reading frame, AUG-stop, induces boron-dependent ribosome stalling and mRNA degradation. Plant Cell 28:2930–2849
43. Tanaka M, Wallace IS, Takano J, Roberts DM, Fujiwara T (2008) NIP6;1 is a boric acid channel for preferential transport of boron to growing shoot tissues in *Arabidopsis*. Plant Cell 20:2860–2875
44. Tanaka M, Takano J, Chiba Y, Lombardo F, Ogasawara Y, Onouchi H, Naito S, Fujiwara T (2011) Boron-dependent degradation of NIP5;1 mRNA for acclimation to excess boron conditions in *Arabidopsis*. Plant Cell 23:3547–3559
45. Warington K (1923) The effect of boric acid and borax on the broad bean and certain other plants. Ann Bot 37:629–672
46. Xu F, Wang Y, Meng J (2001) Mapping boron efficiency gene (s) in *Brassica napus* using RFLP and AFLP markers. Plant Breed 10:31–324
47. Yamaji N, Ma JF (2014) The node, a hub for mineral nutrient distribution in graminaceous plants. Trends Plant Sci 19:556–563
48. Yamaji N, Ma JF (2017) Node-controlled allocation of mineral elements in Poaceae. Curr Opin Plant Biol 39:18–24
49. Yoshinari A, Fujimoto M, Ueda T, Inada N, Naito S, Takano J (2016) DRP1-dependent endocytosis is essential for polar localization and boron-induced degradation of the borate transporter BOR1 in *arabidopsis thaliana*. Plant Cell Physiol 57:1985–2000
50. Zhang Q, Chen H, He M, Zhao Z, Cai H, Ding G, Shi L, Xu F (2017) The boron transporter BnaC4.BOR1;1c is critical for inflorescence development and fertility under boron limitation in *Brassica napus*. Plant Cell Environ 40:1819–1833

Figures

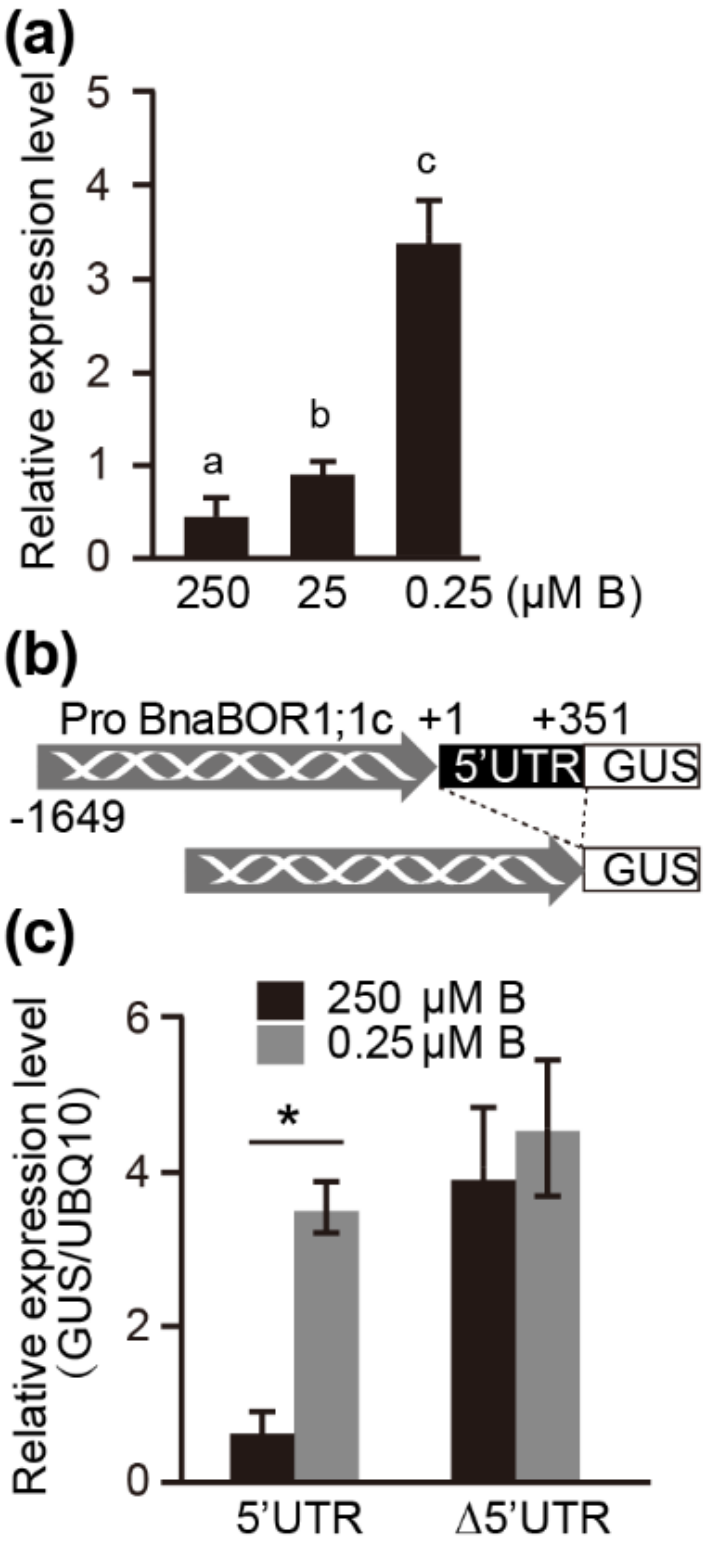

Figure 1

5'-UTR mediates high B response of BnaC4.BOR1;1c. (a) Relative expression levels of BnaC4.BOR1;1c gene in response to low (0.25 μM B), normal (25 μM B), and high B (250 μM B) treatments. Roots of 15-day-old seedlings grown in hydroponic solution with different B supply were used. Values represent

means ± SD (n = 3 independent lines). Different letters indicate significantly different values (one-way ANOVA, Duncan's test). (b) Schematic representations of ProBnaC4.BOR1;1c (5'-UTR):GUS and ProBnaC4.BOR1;1c (Δ5'-UTR): GUS constructs. (c) Relative expression levels of these two constructs in the transgenic Arabidopsis lines responsed to B treatments (0.25 μM B and 250 μM B). 10-d-old Arabidopsis seedlings grown on 100 μM B medium were transferred to 0.25 μM B or 250 μM B medium for 2 d growth. Experiments were performed using 3 independent homozygous lines. Values represent means ± SD (n = 3). * $p < 0.05$, Student's t-test.

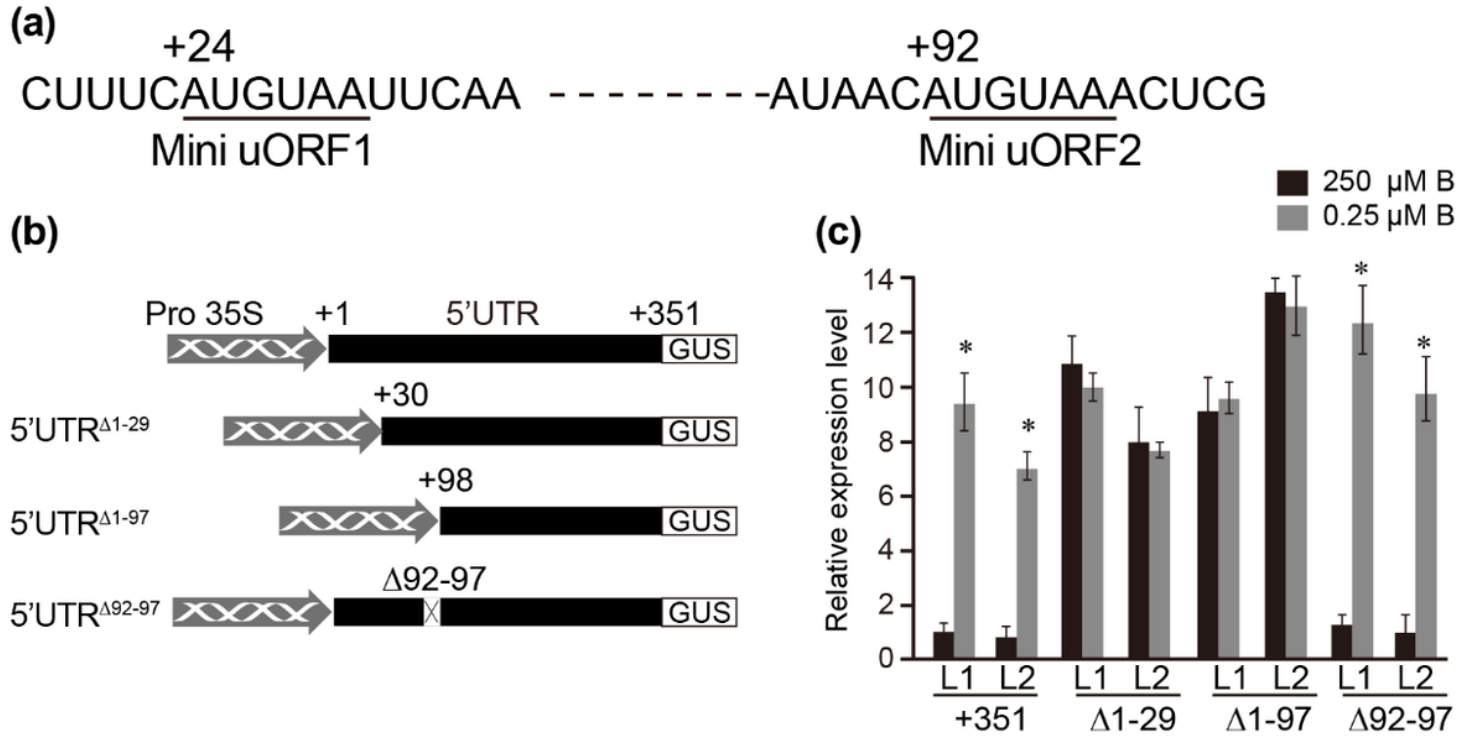

Figure 2

5' terminal region of 5'-UTR is required for high B response of BnaC4.BOR1;1c. (a) Sequences of two mini uORFs (AUGUAA) in 5'-UTR. (b-c) Truncation analyses of 5'-UTR for high B regulation of BnaC4.BOR1;1c. Truncated sequences with deletion of 29 nt, 97 nt, and 92-97 nt in 5'-UTR were fused to 35S promoter to express GUS protein in transgenic Arabidopsis, respectively (b), and their relative expression levels in response to B treatments were investigated (c). 10-d-old Arabidopsis seedlings grown on 100 μM B medium were transferred to 0.25 μM B or 250 μM B medium for 2 d growth. Values represent means ± SD (n = 3). * $p < 0.05$, Student's t-test.

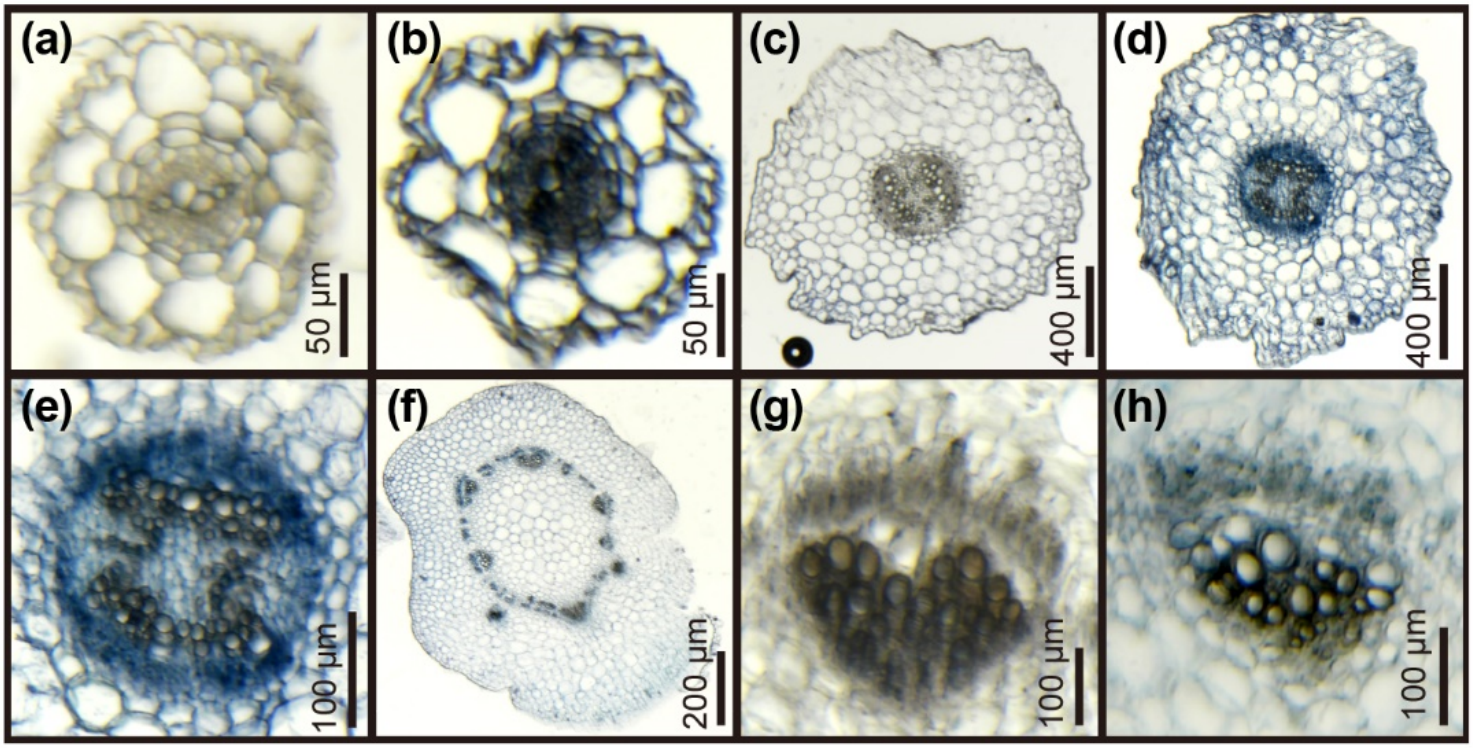

Figure 3

In situ PCR analysis of BnaC4.BOR1;1c in B.napus. In situ PCR analysis was performed in roots (a, b), hypocotyl (c-e), and node (f-h) of B. napus. Negative control in roots (a), hypocotyl (c), and node (g) was prepared due to the reverse transcription PCR without primer supply. 20-d-old B. napus seedlings grown on 25 µM B medium were transferred to 0.25 µM B medium for 2 d growth. Fresh plant tissues were cut and fixed in FAA solution for subsequent in situ PCR analysis.

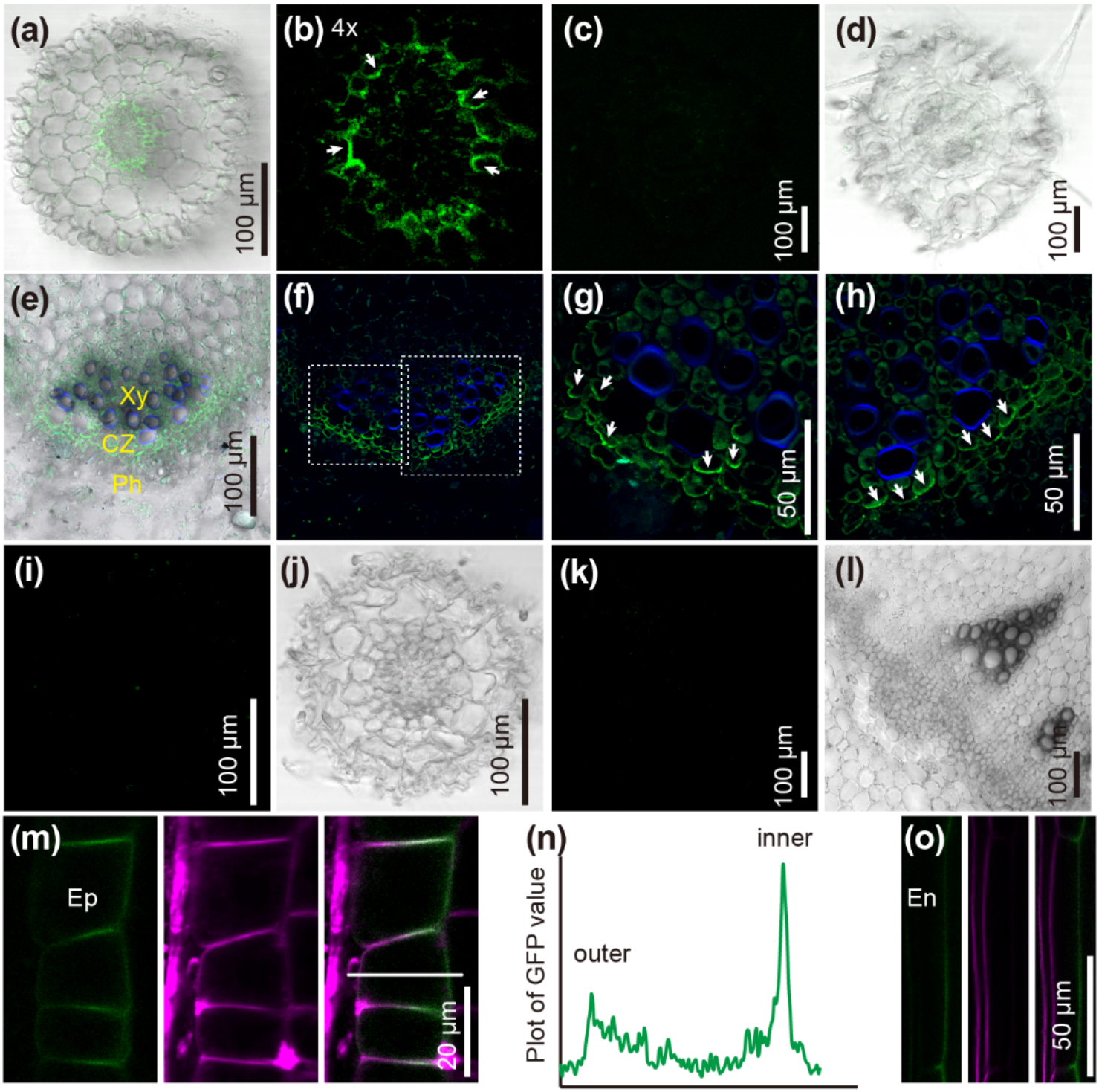

Figure 4

BnaC4.BOR1;1c localizes on the vascular cell layers of tissues. Immunohistological staining of BnaC4.BOR1;1c using specific anti-BnaC4.BOR1;1c antibody in roots and nodes. Roots (a, b) and nodes (e, f) of wild-type B. napus and roots of RNAi plant (c, d) grown in 0.25 μM B were used. (b) close-up view of (a) and (g, h) close-up view of (e) were shown. 250 μM B treated wild-type roots (i, j) and nodes (k, l) were used to inhibit BnaBOR1s expression in B. napus. Xy, xylem; CZ, cambium; Ph, Phloem. Localization analysis of Arabidopsis expressing 35s: BnaC4.BOR1;1c-GFP in epidermis (m) and endodermis (o). FM4-

64 (magenta) was used to stain the plasma membrane. The GFP signal intensity on the plasma membrane toward the soil-side (outer) and the stele-side (inner) was quantified by line plot (n). Ep, epidermis; En, endodermis.

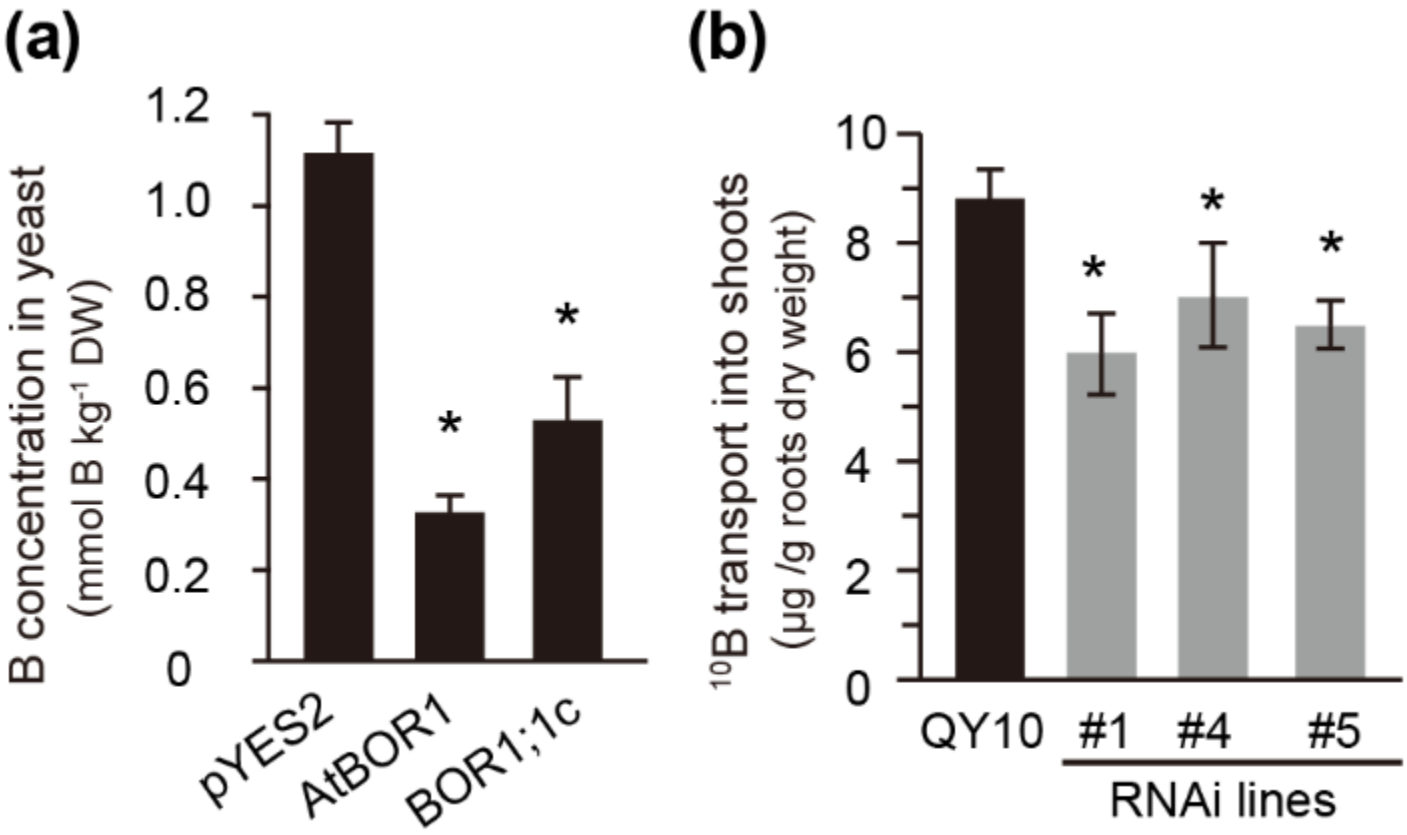

Figure 5

BnaC4.BOR1;1c transport B in yeast and B. napus. (a) Yeasts were incubated in 500 µM B for 60 min in galactose medium. The B intracellular concentrations in yeast expressing 3 vectors above were measured. Values represent means ± SD (n = 3). (b) Comparison of transient B uptake in 'QY10' and BnaC4.BOR1;1c RNAi lines. 10-day-old seedlings grown on 100 µM 11B enriched hydroponic solution was treated in 0.25 µM 11B for 1 day followed by 1-day growth in 5 µM 10B-enriched hydroponic solution. Values represent means ± SD (n = 3).

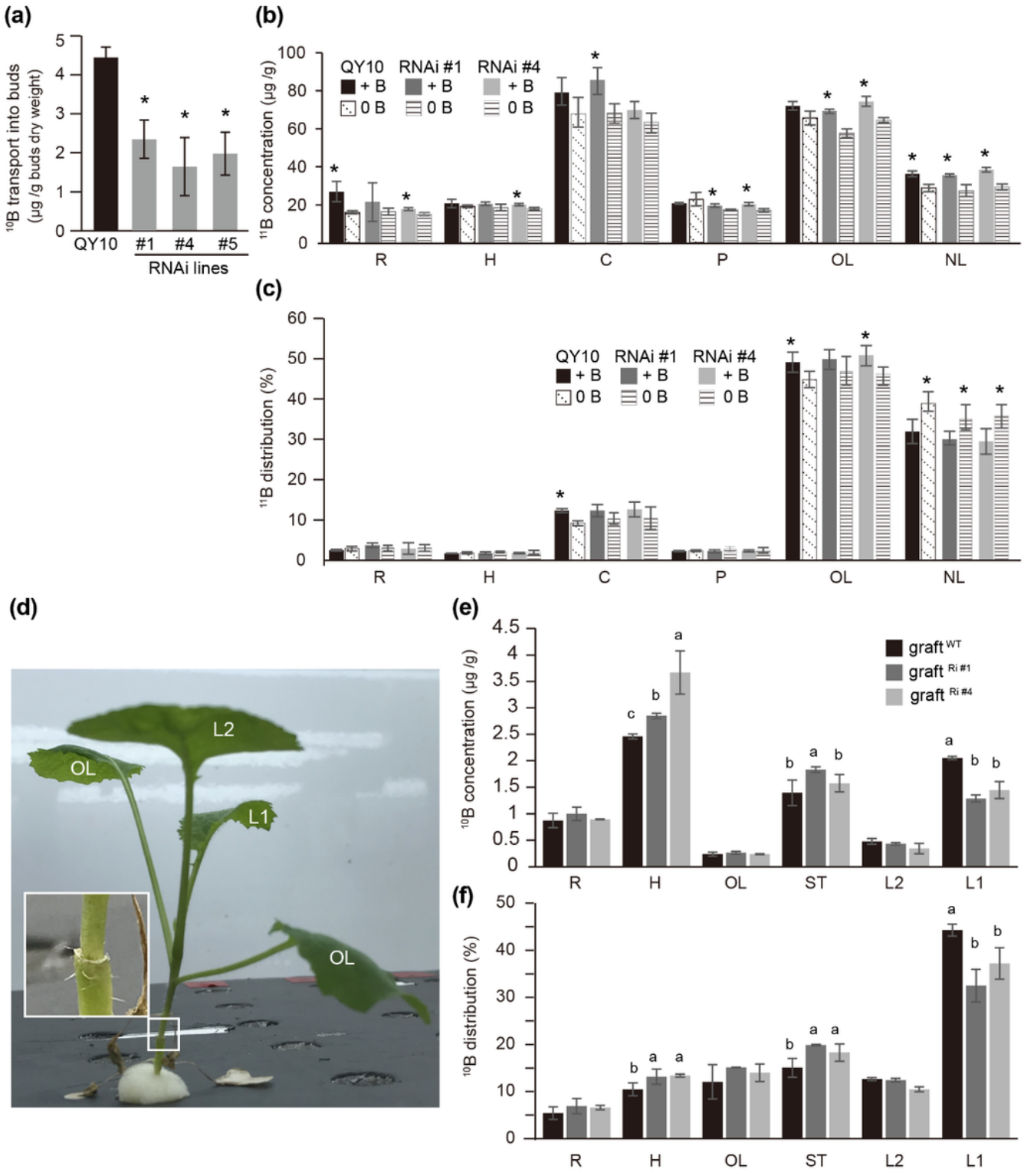

Figure 6

BnaC4.BOR1;1c preferentially transport B into developing tissues under B deficiency. (a) Comparison of transient B uptake in 'QY10'and BnaC4.BOR1;1c RNAi lines. Inflorescences cut from plants grown in a pot with 100 μM 11B irrigation were cultured 2 days in a hydroponic box with 5 μM 10B. (b, c) Comparison of B centration and B distribution ratio in 'QY10' and BnaC4.BOR1;1c RNAi lines. 22-day-old seedlings (4 true leaves stage) grown on 100 μM 11B-enriched hydroponic solution was treated with B deprivation for 2

days. Tissues for B concentration measurement were sampled before B deprivation (+ B) and after B deprivation (0 B). Significant differences between + B and 0 B were statistically analyzed. Values represent means ± SD (n = 3). *: $p < 0.05$, Student's t-test. (d) Chimera plants generation. Scions of 15-day-old 'QY10' and RNAi lines were inserted into 'QY10' rootstock to produce graftWT, graftRi#1, and graftRi #4. High humidity is required to maintain a high survival ratio. The leaves order was indicated in (d). (e-f) Comparison of transient B uptake and B distribution ratio in chimera plants. Chimera plants grown in100 μM 11B-enriched solution were transferred to 0.1 μM 11B-enriched medium for 1 day followed by 2 days exposure in 1 μM 10B-enriched solution. Tissues for B concentration measurement were sampled before and after 10B treatment. Values represent means ± SD (n = 3). Different letters indicate significantly different values (one-way ANOVA, Duncan's test). R: root; H: hypocotyl; C: cotyledon; P: petiole; OL: old leaves; NL: new leaves; ST: stem.

Supplementary Files

This is a list of supplementary files associated with this preprint. Click to download.

- FigureS.docx
- Primers.docx